arXiv:2208.03186v6 [hep-ph] 1 Jun 2023

Gluon gravitational form factors of protons from charmonium photoproduction

Xiao-Yun Wang,[1,2,*] Fancong Zeng,[3,4,†] and Quanjin Wang[1]

[1]*Department of physics, Lanzhou University of Technology, Lanzhou 730050, China*
[2]*Lanzhou Center for Theoretical Physics, Key Laboratory of Theoretical Physics of Gansu Province, Lanzhou University, Lanzhou, Gansu 730000, China*
[3]*Institute of High Energy Physics, Chinese Academy of Sciences, Beijing 100049, China*
[4]*University of Chinese Academy of Sciences, Beijing 100049, China*

(Dated: June 2, 2023)

Inspired by the recent near-threshold J/ψ photoproduction measurements, we discuss gluon gravitational form factors (GFFs) and internal properties of the proton. This work presents a complete analysis of the proton gluon GFFs connecting the gluon part of the energy-momentum tensor and the heavy quarkonium photoproduction. In particular, a global fitting of the J/ψ differential and total cross section experimental data is used to determine the gluon GFFs as functions of the squared momentum transfer t. Combined with the quark contributions to the D-term form factor extracted from the deeply virtual Compton scattering experiment, the total D-term is obtained to investigate their applications in describing the proton mechanical properties. These studies provide a unique perspective on investigating the proton gluon GFFs and important information for enhancing QCD constraints on the gluon GFFs.

I. INTRODUCTION

The form factor provides critical information about many fundamental aspects of hadron structure. While the weak and electromagnetic form factors of the proton are well-established, our understanding on gravitational form factors (GFFs) is incomplete. The GFFs are defined from matrix elements of the quantum chromodynamics (QCD) energy-momentum tensor (EMT) and provide direct access to the internal structure of the proton, including its mass, spin, and mechanical properties [1, 2]. The sum contributions of the quark and gluon GFFs are measurable quantities defined purely from the internal system, which describes the internal dynamics of the proton system [3].

The GFFs, including the D-form factor, have also been studied in numerous frameworks Recently, the quark D-form factor $D_q(t)$ has been extracted from the deeply virtual Compton scattering (DVCS) experiments at the Thomas Jefferson National Accelerator Facility (JLab), and the pressure distribution inside the proton has been reported [4]. However, because the DVCS is almost insensitive to gluons, the gluon D-form factor is controversial and seldom extracted. On the theoretical side, one study obtained the proton GFFs and investigated the mechanical properties using a light-front quark-diquark model constructed by the soft-wall AdS/QCD [5]. The nucleon form factors of the EMT are studied in the framework of the Skyrme model and in-medium modified Skyrme model [6, 7]. Reference [8] demonstrated the pressure, energy density, and mechanical radius of the nucleon in light-cone QCD sum rule formalism. On the other hand, the distributions of pressure and shear forces inside the proton are investigated with lattice QCD calculations [3, 9, 10], enhancing our understanding of the proton GFFs.

Unfortunately, there are no experimental constraints on the gluon GFFs directly, and little information about the gluon GFFs is explicit at present. However, at finite momentum transfer, the near-threshold heavy quarkonium photoproduction, such as J/ψ and Υ meson, offers a superior path to access the gluon GFFs [11–19]. These processes have gained quite an interest in recent years because they promise to measure the naturalness of proton mass decomposition [17–21]. One reason is that the scalar gluon operator is dominant in the production amplitude of heavy quarkonium. Moreover, heavy vector mesons photoproduction was employed because the high mass of J/ψ limits the interaction to a short distance. In electroproduction the short distance is given when $Q^2 >> 1$ GeV^2, i.e. high photon virtuality. These facts allow us to discuss the gluon GFFs by studying the near-threshold photoproduction data of heavy quarkonium. Conversely, the connection between heavy quarkonium photoproduction and gluon GFFs also faces challenges. One study revealed that this process is light-cone dominated and has no direct connection with gluon GFFs [22]. Thereby, more theoretical research on the related physical mechanisms is still needed.

Therefore, experimental information on vector meson photoproduction is essential to gain insight into the gluon GFFs of the proton. Recently, the GlueX Collaboration reported the near-threshold cross section of the reaction $\gamma p \to J/\psi p$ [23]. The JLab experiment measured the differential cross section of J/ψ on proton targets at a photon energy E_γ from 9.1 GeV to 10.6 GeV [11], which is a near-threshold energy region. Those experimental data offer a good window for studying the internal character of the proton. Currently, there are plans for future experiments at JLab and Electron Ion Colliders (EICs) to probe the deepest structure inside the proton and collect J/ψ data [24–26]. High-precision experimental measurements are suggested to be performed at these facilities.

This paper is organized as follows. In Sec. II, we provide a formulas for connecting the photoproduction and gluon GFFs, and the process of calculating the proton internal properties. In Sec. III, we determine the gluon GFFs by global fitting the differential and total cross section of J/ψ photoproduction. Subsequently, the computation result of the mechanical properties and energy property inside the proton is presented.

* xywang@lut.edu.cn
† zengfc@ihep.ac.cn

A summary is given in Sec. IV.

II. FORMALISM

A. the photoproduction and gluon GFFs

The (00) component of the EMT defines the isotropous form factor in the Breit frame, which can be expressed as follows. [1, 20, 27, 28]

$$\langle P'|T_{00}|P\rangle = \bar{u}(P')u(P)G(t) \tag{1}$$

where the spinor normalization $\bar{u}(P')u(P) = 2M$ and M is the proton mass. $G(t)$ is the proton GFFs, which are parametrized as follows. [1, 20]

$$G(t) = MA_{q+g}(t) + \frac{t}{4M}B_{q+g}(t) - \frac{t}{4M}D_{q+g}(t) \tag{2}$$

where $t = -Q^2$ is the squared momentum transfer, the form factor $B_{q+g}(t) = 2J_{q+g}(t) - A_{q+g}(t)$ is consistent with zero basically [9, 16, 29]. The form factors $A_{q+g}(t)$, $J_{q+g}(t)$ and $D_{q+g}(t)$ provide the information about the mass, spin and the mechanical properties of the proton, respectively.

The proton GFFs are the sum contributions of the quark and gluon GFFs.Additionally, the component of the gluon GFFs part can be written as follows. [1]

$$\begin{aligned} G_g(t) =& MA_g(t) - \frac{t}{4M}\Big(-B_g(t) + D_g(t)\Big) + M\bar{C}_g(t) \\ =& \frac{3}{4}MA_g(t) - \frac{t}{4M}D_g(t) + \frac{3t}{16M}\Big(B_g(t) + D_g(t)\Big) \end{aligned} \tag{3}$$

because the $\bar{C}_g(t)$ form factor can be written as [30]

$$\bar{C}_g(t) = -\frac{A_g(t)}{4} + \frac{-t}{16M^2}\Big(B_g(t) - 3D_g(t)\Big)$$

here, the constraint $\bar{C}_g(t) + \bar{C}_q(t) = 0$ is due to EMT conservation [1].

Many estimatations or models, including QCD sum rule [31, 32], Braun-Lenz-Wittman model, [32] and the asymptotic model [30], show that the $B_g(t)+D_g(t)$ are order of magnitudes smaller compared to the $B_g(t)$ or $D_g(t)$ results [30]. In this paper, we mainly attribute the gluon GFFs to the first two terms in Eq. 4, as the contribution of the $B_g(t) + D_g(t)$ is negligible. Therefore, the gluon GFFs are obtained as follows:

$$G_g(t) \approx \frac{3}{4}MA_g(t) - \frac{t}{4M}D_g(t) \tag{4}$$

Next, we demonstrate the complete analysis of the proton gluon GFFs connecting the gluon part of the EMT and the near-threshold J/ψ cross section. Typically, the differential cross section of the J/ψ photoproduction is given by [33]

$$\frac{d\sigma_{\gamma p\to J/\psi p}}{dt} = \frac{1}{64\pi W^2}\frac{1}{|\mathbf{p}_\gamma|^2}\left|\mathcal{M}_{\gamma p\to J/\psi p}\right|^2 \tag{5}$$

where W is the center of mass (c.m.) energy and $\mathbf{p}_\gamma$ is the c.m. photon momentum in the $\gamma p \to J/\psi p$ process. As an assumption, the amplitude primarily attributes to the gluon part of the EMT of QCD in this paper, which can be written as follows. [13]

$$\mathcal{M}_{\gamma p\to J/\psi p} = -2c_2Q_cM\left\langle P'|g^2T^g_{00}|P\right\rangle \tag{6}$$

where $Q_e = 2e/3$ represents the coupling of the photon to the electric charge of the quarks in J/ψ meson; c_2, the short-distance coefficient, is on the order of $\pi r^2_{c\bar{c}}$; and $g^2 = 4$ is the QCD coupling with $\alpha_s \approx 0.32$ [18, 34].

By integrating the differential cross section (Eq. 5) over the allowed kinematical range from t_{min} to t_{max}, the total cross section are computed and can be written as follows.

$$\sigma = \int_{t_{min}}^{t_{max}} dt\left(\frac{d\sigma}{dt}\right), \tag{7}$$

here, the limiting values t_{min} and t_{max} are

$$t_{max}(t_{min}) = m^2_{J/\psi} - 2E_\gamma E_{J/\psi} \pm 2|\mathbf{p}_\gamma||\mathbf{p}_{J/\psi}|. \tag{8}$$

The energies and momenta of the photon and vector meson in the c.m. frame are

$$\begin{aligned} |\mathbf{p}_{J/\psi}| &= \frac{1}{2W}\sqrt{(W^2-M^2)^2 + m^2_{J/\psi}(m^2_{J/\psi} - 2W^2 - 2M^2)}, \\ E_{J/\psi} &= \sqrt{|\mathbf{p}_{J/\psi}|^2 + m^2_{J/\psi}}, \quad |\mathbf{p}_\gamma| = \frac{1}{2W}(W^2-M^2), \quad E_\gamma = |\mathbf{p}_\gamma|. \end{aligned} \tag{9}$$

Thus far, we have established the relationship between the proton GFFs and J/ψ photoproduction, including the differential and total cross section in Eqs. 5 and 7.

For $A_{q+g}(t)$, the mass distribution of the proton is encoded in the A-form factor, which can be expressed under the dipole form parametrization as follows.

$$A_{q+g}(t) = \frac{A_q(0)}{(1-t/m_q^2)^2} + \frac{A_g(0)}{(1-t/m_g^2)^2} \tag{10}$$

where the constraint $A_q(0) + A_g(0) = 1$ is the consequence of momentum conservation [1, 35]. Moreover, the gluon contribution $A_g(0) = 0.414$ was obtained from CT18 global QCD analysis [36], and agrees with other LQCD results [10, 37, 38]. Therefore, the parameter $A_g(0)$ in $A_g(t)$ is fixed in this study, and m_g is a free parameter determined by fitting experimental data.

The D-form factor $D_{q+g}(t)$ is an area of significant interest, which has attracted considerable attention recently [1, 11]. The gluon D-form factor $D_g(t)$ is typically parameterized in the tripole form and provided as follows. [4, 39]

$$D_g(t) = \frac{D_g(0)}{(1-t/d_g^2)^3} \tag{11}$$

where $D_g(0)$ and d_g are free parameters adjusted to the experimental data. Note that $D_g(0)$ is negative as the pressure distribution is found to be repulsive near the proton center.

It has been determined that the form factor $G(t)$ in Eq. 2 and 4 at the momentum transfer t=0 satisfies

$$G(0) = M \quad \text{and} \quad G_g(0) = \frac{3}{4} M A_g(0) \tag{12}$$

Therefore, the coefficient c_2 can be determined by extracting the near-threshold differential cross section at t=0, which can be written as follows.

$$\left.\frac{d\sigma_{\gamma p\to J/\psi p}}{dt}\right|_{t=0} = \frac{1}{64\pi W^2}\frac{1}{|\mathbf{p}_\gamma|^2}\left|3c_2 Q_c g^2 M^3 A_g(0)\right|^2 \tag{13}$$

As the differential cross section at squared momentum transfer t=0 is nonphysical with no experimental measurement, we will identify the left side of Eq. 13 at different c.m. energy based on the model prediction as discussed in Ref. [40], which is described in detail in Sec. III. As a result, reliable gluon GFFs can be obtained while avoiding the c.m. energy dependence caused by the differential cross sections at varying photon energies. This approach provides significant information on the gluon GFFs.

Finally, we construct the relationship between the gluon GFFs of the proton and the near-threshold heavy quarkonium photoproduction. Thus one can derive the gluon GFFs, which is the joint effect of J/ψ differential and total cross section.

B. proton internal properties

The pressure $p(r)$ and shear forces $s(r)$ are "good observables" to report the pressure and shear forces distributions, indicating that the average value of the directional static pressure and shear forces along the three Cartesian axes can be expressed as follows. [1, 2]

$$s_{q+g}(r) = -\frac{1}{2} r \frac{d}{dr}\frac{1}{r}\frac{d}{dr}\widetilde{D}(r) \tag{14}$$

$$p_{q+g}(r) = \frac{1}{3}\frac{1}{r^2}\frac{d}{dr} r^2 \frac{d}{dr}\widetilde{D}(r) \tag{15}$$

Here $\widetilde{D}(r)$ is the Fourier transform of $D_{q+g}(t)$ and can be expressed as follows. [1, 2]

$$\begin{aligned}\widetilde{D}(r) &= \int \frac{d^3\mathbf{\Delta}}{2M(2\pi)^3} e^{-i\Delta r} D_{q+g}(-\mathbf{\Delta}^2) \\ &= \int \frac{d^3\mathbf{\Delta}}{2M(2\pi)^3} e^{-i\Delta r}\left(D_g(-\mathbf{\Delta}^2) + D_q(-\mathbf{\Delta}^2)\right)\end{aligned} \tag{16}$$

Note that the pressure distribution $r^2 p_{q+g}(r)$ satisfies the internal forces balance inside a composed particle based on [1]

$$\int_0^\infty dr\, r^2 p_{q+g}(r) = 0 \tag{17}$$

The normal forces in the composed particle system can be written as [1]

$$F_n(r) = \frac{2}{3} s_{q+g}(r) + p_{q+g}(r) \tag{18}$$

here the positive and negative eigenvalues correspond to "stretching" or "squeezing" along the corresponding principal axes, respectively. The normal forces satisfy $F_n(r) > 0$ [1]. One can define the proton mechanical radius in terms of the normal forces in the proton, which can be written as [1]

$$\left\langle R^2_{mech}\right\rangle = \frac{\int d^3r\, r^2 F_n^{q+g}(r)}{\int d^3r\, F_n^{q+g}(r)} = \frac{12\left(\frac{D_q(0)}{d_q} + \frac{D_g(0)}{d_g}\right)}{D_q(0)d_q + D_g(0)d_g} \tag{19}$$

After calculating the form factor $D_{q+g}(t)$, the pressure in the proton center can be computed directly as [1]

$$p(0) = \frac{1}{24\pi^2 M}\int_{-\infty}^{0} -(-t)^{3/2} D_{q+g}(t)dt \tag{20}$$

which is consistent with the illustration in Eq. 15.

The total energy density $T_{00}(r)$ satisfied $T_{00}(r) > 0$ in a mechanical system is defined for the total system in Eqs. 1 and 2, which can be written as [1]

$$\begin{aligned}T_{00}(r) &= \int \frac{d^3\mathbf{\Delta}}{(2\pi)^3} e^{-ir\Delta}\left(MA_{q+g}(t) - \frac{t}{4M} D_{q+g}(t)\right) \\ &= \sum_{a=q,g} \frac{16M^2 A_a(0) m_a^3 e^{-m_a r} - (-3 + d_a r) D_a(0) d_a^5 e^{-d_a r}}{128\pi M}\end{aligned} \tag{21}$$

where $-\mathbf{\Delta}^2 = t$. The total energy density $T_{00}(r)$ satisfy the following condition:

$$\begin{aligned}\int d^3r T_{00}(r) &= \int d^3r\left(T^g_{00}(r) + T^q_{00}(r)\right) \\ &= M\left(A_q(0) + A_g(0)\right) = M\end{aligned} \tag{22}$$

The energy density satisfies $T_{00}(r) > 0$ in a mechanical system, allowing us to introduce the mean square radius of the energy density as follows. [1]

$$\left\langle R^2_E\right\rangle = \frac{\int d^3r r^2 T_{00}(r)}{\int d^3r T_{00}(r)} = 6A'_{q+g}(0) - \frac{3\left(D_0 + d(0)\right)}{2M^2} \tag{23}$$

III. RESULTS AND DISCUSSION

In our previous work [40], the analysis revealed that certain light quarks are strongly suppressed in heavy quarkonium photoproduction and are likely to dominate the two-gluon exchange mechanisms. The obtained numerical results showed that the two-gluon exchange model can explain the near-threshold J/ψ photoproduction experimental data well [40]. Consequently, the differential cross section $d\sigma/dt|_{t=0}$ in Eq. 13 at various c.m. energy is predicted by the two-gluon exchange model, allowing the identification of the corresponding short-distance coefficient c_2 can be identified. Additionally, the introduction of the model is helpful for obtaining a continuous total cross section. Subsequently, the gluon GFFs in Eq. 4 are achieved through fitting Eqs. 5 and 7 simultaneously. By global fitting the near-threshold t-dependence J/ψ differential cross section and W-dependence total cross

section experimental data [11, 23, 41–44], the free parameters m_g, d_g and $D_g(0)$ in Eq. 4 are computed. The differential and total experimental data used in this study are derived from the experiment results that are currently closest to the threshold. The comparison between the J/ψ photoproduction (blue solid curves) and experimental measurements (black points) are presented in Figs. 1 and 2, showing a good agreement. The blue bands reflect a statistical error of parameters m_g, d_g, and $D_g(0)$. The results of holographic QCD and the GPD+VMD approach were recalculated in Ref. [11] using the latest differential cross section data. The obtained gluon GFFs are compared to that of the holographic QCD, the GPD+VMD approach, and LQCD [9–12, 19], as presented in Table I. Notably, our results are comparable to that of holographic QCD determination and LQCD calculation.

As shown in Fig. 3, the values of gluon A-form factor $A_g(t)$ (red dashed curve) and gluon D-form factor $D_g(t)$ (blue solid curve) are compared with the LQCD determinations [10]. Here the error of parameters m_g, $D_g(0)$ and d_g include all uncertainties of $A_g(t)$ and $D_g(t)$. One finds that the results obtained for gluon D-form factor in this work is comparable with that obtained from the LQCD computations, while the values of $A_g(t)$ is bigger than the LQCD results slightly. We have also compared the gluon D-form factor with the quark counterparts extracted from the DVCS experiment, and as a result, the gluon and quark D-form factor are approximately comparable, which is in agreement with numerous previous studies [4, 9, 10].

The sum of the quark and gluon D-form factors $D_{g+q}(t)$ is a measurable quantity defined solely by the D-term inside the proton. Particularly, one can obtain the quark D-form factor by fitting the DVCS data [4] using the tripole form presumption [39]. Combined with the gluon D-term achieved in this work, one can obtain the proton mechanical properties from $D_{g+q}(t)$, including the quark and gluon contributions.

The pressure and shear forces distributions inside the proton are achieved and displayed in Fig. 4. The red-dashed and blue-solid curves indicate the gluon and quark contributions of the pressure and shear forces distributions, respectively. The blue and green bands represent the uncertainties that come from the error of the parameters d_g and $D_g(0)$. Here,the positive sign indicates repulsion toward the outside, and the negative sign indicates attraction directed towards the inside. The total pressure and shear forces contributions for the sum of the quark and gluon contributions are illustrated as the green-dot-dashed curve in Fig. 4. It was found that the pressure is positive in the inner region and negative in the outer region, with a zero crossing near $r = 0.67$ fm, which shows that the repulsive and binding pressures dominate in the proton and are separated in radial space. Moreover, the shear forces distribution reaches its peak near $r = 0.63$ fm in our observation.

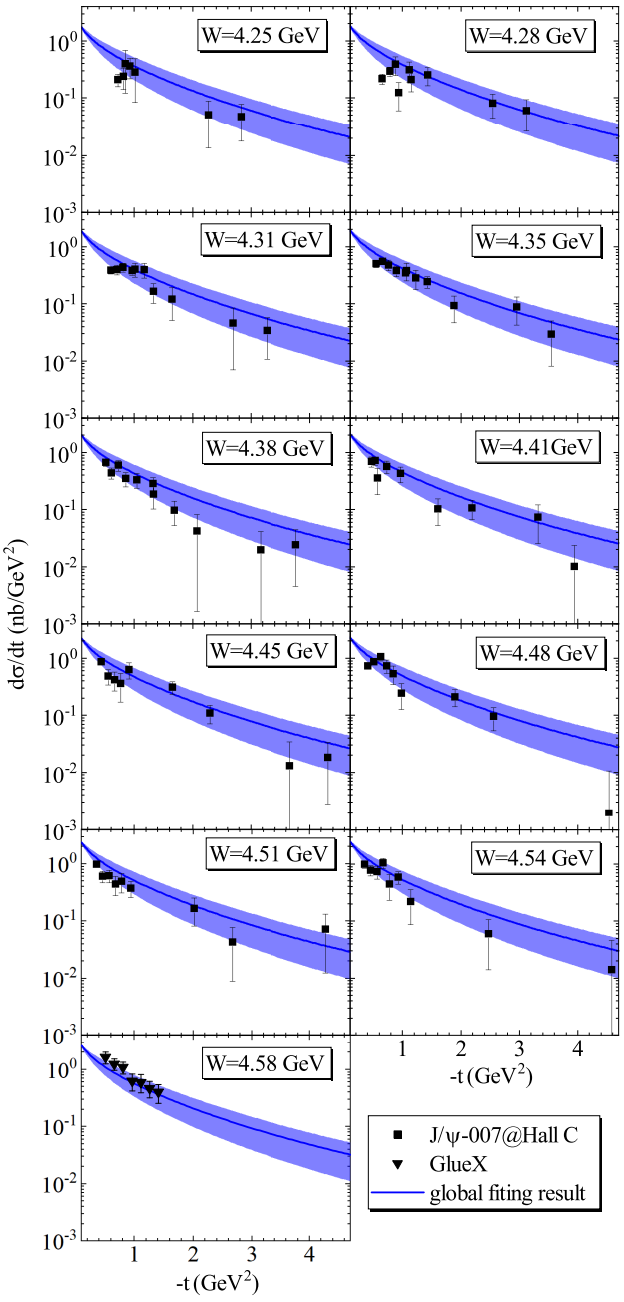

FIG. 1. Global fitting result of $\gamma p \to J/\psi p$ differential cross section as a function of $-t$ at c.m. energy $W = 4.25$ GeV, 4.28 GeV, 4.31 GeV, 4.35 GeV, 4.38 GeV, 4.41 GeV, 4.45 GeV, 4.48 GeV, 4.51 GeV, 4.54 GeV and 4.58 GeV. The blue bands reflect statistical error of m_g, d_g and $D_g(0)$. References of data can be found in [11, 23].

After discussing the gluon form factors $A_g(t)$ and $D_g(t)$, the gluonic contribution to the nucleon mechanical properties can be achieved. An important mechanical quantity, known as $p_g(0)$, denotes the pressure of the gluon contribution in the center of the nucleon and has a of $0.62^{+0.42}_{-0.27}$ GeV/fm^3. One can add the quark contribution $p_q(0) = 0.93$ GeV/fm^3 and

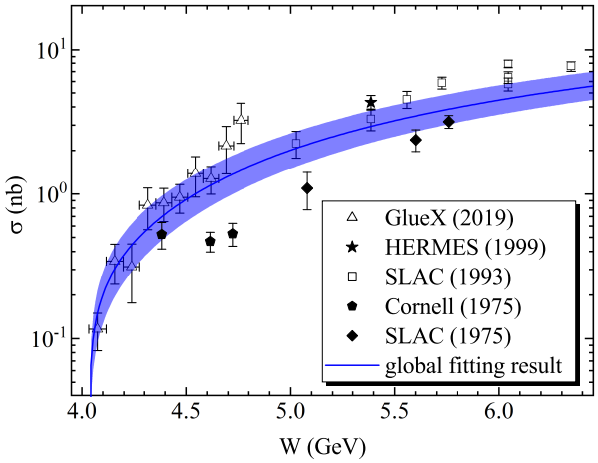

FIG. 2. Global fitting result of $\gamma p \to J/\psi p$ total cross section as a function of c.m. energy W. The blue band reflects statistical error of m_g, d_g, and $D_g(0)$. References of data can be found in [23, 41–44] .

TABLE I. Parameters m_g, $D_g(0)$ and d_g by a global fitting of the differential and total cross section experimental data [11, 23, 41–44], compared with the holographic QCD, the GPD+VMD approach and LQCD results [9–12, 19].

approach	m_g (GeV)	D_0	d_g (GeV)
Holographic QCD [11, 12] tripole-tripole	1.575	-1.80 ± 0.528	1.21 ± 0.21
GPD + VMD [11, 19] tripole-tripole	2.71	-0.80 ± 0.44	1.28 ± 0.50
LQCD [9] tripole-tripole	1.641	-1.932 ± 0.532	1.07 ± 0.12
LQCD [10] dipole-dipole	1.13	-10.0	0.48
this work dipole-tripole	1.51 ± 0.10	-1.97 ± 0.25	0.86 ± 0.07

compute the system pressure $p(0) = 1.55^{+0.42}_{-0.27}$ GeV/fm^3 at the center of the proton. Moreover, the proton mechanical radius is computed to be $0.75^{+0.04}_{-0.03}$ fm. As listed in Table II, those proton mechanical quantities are compared with other existing theoretical results. As shown in Table II, our statements on the pressure density differ from the findings in previous studies considerably [7, 8, 45–47]. In fact, the quark contribution to the pressure is bigger than most of those reported previously, regardless of the gluon contribution. The calculation of mechanical radius is consistent with the result reporetd in Refs. [3, 8, 45, 47], subjected to the error margin.

IV. SUMMARY

This work constructs a connection between the gluon part of EMT and the near-threshold charmonium photoproduction.

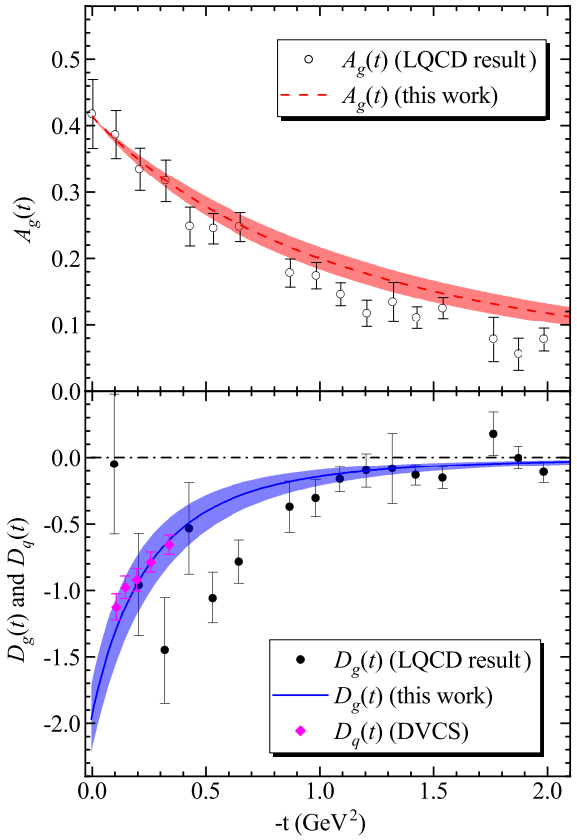

FIG. 3. Top panel: The gluon A-form factor $A_g(t)$ (red-dashed curve) compared with the LQCD determinations [10]. Bottom panel: The gluon D-form factor $D_g(t)$ (blue-solid curve) compared with the LQCD determinations [10] and the quark D-form factor from DVCS enperiment [4]. The blue band reflects an statistical error of the parameters m_g, $D_g(0)$ and d_g.

TABLE II. Numerical values of mechanical quantities of proton, including the proton mechanical radius and the pressure at the center of the proton, compared with other predictions from different approaches.

Approaches and Models	$p(0)$ (GeV/fm^3)	$\sqrt{\langle R^2_{mech} \rangle}$ (fm)
light-front quark-diquark model [46]	4.76	0.50
Skyrme model [7]	0.26	-
light-cone QCD [8]	0.67	0.73
light-cone sum rules at leading order [45]	0.84	0.72
lattice QCD (modified z-expansion) [3]	-	0.71
lattice QCD (tripole ansatz) [3]	-	0.75
$\pi - \rho - \omega$ soliton model [47]	0.58	-
this work	$1.55^{+0.42}_{-0.27}$	$0.75^{+0.04}_{-0.03}$

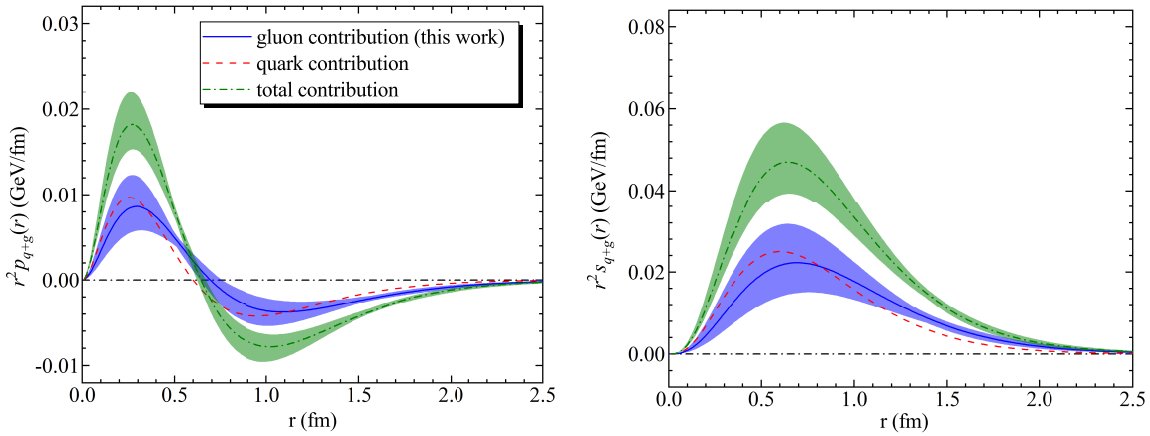

FIG. 4. Left panel: The pressure distribution $r^2 p(r)$ inside the proton. Right panel: The shear force distribution $r^2 s(r)$ inside the proton. The red-dashed and blue-solid curve shows the quark and gluon contributions, respectively. The green-dot-dashed curve represents the total pressure and shear forces distributions. The blue and green band cover all the statistical uncertainties of $D_g(0)$ and d_g.

The gluon GFFs, as functions of the squared momentum transfer t, are determined by a global fitting of the J/ψ differential and total cross section experimental data. All gluon form factors $A_g(t)$, $B_g(t)$, $D_g(t)$ and $\bar{C}_g(t)$, which are related to different components of the gluon GFFs, are resolved. One finds that $D_g(t)$ is comparable with the lattice QCD results, while the value of $A_g(t)$ is slightly bigger than the holographic QCD and LQCD results. Subsequently, the gluon contribution of the energy density in the center of the proton, which are determined by both $A_g(t)$ and $D_g(t)$, is calculated. Combined with the quark D-form factor extracted from the DVCS experiment, the total D-term $D_{q+g}(t)$ can be used to investigate its potential applications in describing the mechanical properties. Consequently, the pressure and shear forces distributions inside the proton, including the gluon and quark contributions, are obtained.

It has been suggested that the value of the proton charge radius is [33]

$$R_C = 0.8409 \text{ fm}$$

The proton mechanical radius we obtained is estimated to be $0.75^{+0.04}_{-0.03}$ fm, which is slightly less than the charge radius. Generally, the measurements of the charge distribution and the mechanical properties of the proton can contribute to our understanding of the origin of the proton structure. This study provides useful theoretical insights for the QCD constraints on the gluon GFFs of the proton.

In fact, the dipole and tripole form are typically considered in the $A_{q+g}(t)$ and $D_{q+g}(t)$ form factors, allowing for feasible fitting results in this study. Moreover, this ansatz of the gluon GFFs is convenient to compare with the quark GFFs and other theoretical studies. Nevertheless, it may be feasible to achieve global fitting using artificial neural networks or Schlessinger Point Method [48–50]. Additionally, these new approaches can investigate the model outcomes for $d\sigma/dt|_{t=0}$. Therefore, this work is only the first step, and we will optimize the computational methods in future studies.

The high-precision photo/electroproduction data of vector mesons serve as a crucial foundation for the accurate study of the internal structural properties of the proton. As a result, we recommend relevant experimental measurements based on our findings to be conducted at JLab [23] or EICs [24, 25] facilities.

V. ACKNOWLEDGMENTS

This work is supported by the National Natural Science Foundation of China under Grant Nos. 12065014 and 12047501, and by the Natural Science Foundation of Gansu province under Grant No. 22JR5RA266. We acknowledge the West Light Foundation of The Chinese Academy of Sciences, Grant No. 21JR7RA201.

[1] M. V. Polyakov and P. Schweitzer, "Forces inside hadrons: pressure, surface tension, mechanical radius, and all that," Int. J. Mod. Phys. A **33**, 26, 1830025 (2018).

[2] M. V. Polyakov, "Generalized parton distributions and strong forces inside nucleons and nuclei," Phys. Lett. B **555**, 57-62 (2003).

[3] P. E. Shanahan and W. Detmold, "Pressure Distribution and Shear Forces inside the Proton," Phys. Rev. Lett. **122**, 072003 (2019).

[4] V. D. Burkert, L. Elouadrhiri and F. X. Girod, "The pressure distribution inside the proton," Nature **557**, 7705, 396-399 (2018).

[5] D. Chakrabarti, C. Mondal, A. Mukherjee, S. Nair and X. Zhao, "Gravitational form factors and mechanical properties of pro-

ton in a light-front quark-diquark model," Phys. Rev. D **102**, 113011 (2020).

[6] C. Cebulla, K. Goeke, J. Ossmann and P. Schweitzer, "The Nucleon form-factors of the energy momentum tensor in the Skyrme model," Nucl. Phys. A **794**, 87-114 (2007).

[7] H. C. Kim, P. Schweitzer and U. Yakhshiev, "Energy-momentum tensor form factors of the nucleon in nuclear matter," Phys. Lett. B **718**, 625-631 (2012).

[8] K. Azizi and U. Özdem, "Nucleon's energy–momentum tensor form factors in light-cone QCD," Eur. Phys. J. C **80**, 104 (2020).

[9] P. E. Shanahan and W. Detmold, "Gluon gravitational form factors of the nucleon and the pion from lattice QCD," Phys. Rev. D **99**, 014511 (2019).

[10] D. A. Pefkou, D. C. Hackett and P. E. Shanahan, "Gluon gravitational structure of hadrons of different spin," Phys. Rev. D **105**, 054509 (2022).

[11] B. Duran, Z. E. Meziani, S. Joosten, M. K. Jones, S. Prasad, C. Peng, W. Armstrong, H. Atac, E. Chudakov and H. Bhatt, *et al.* "Determining the gluonic gravitational form factors of the proton," Nature **615**, 7954, 813-816 (2023).

[12] K. A. Mamo and I. Zahed, "J/ψ near threshold in holographic QCD: A and D gravitational form factors," Phys. Rev. D **106**, 086004 (2022).

[13] D. E. Kharzeev, "Mass radius of the proton," Phys. Rev. D **104**(5), 054015 (2021).

[14] X. Ji, Y. Liu and I. Zahed, "Mass structure of hadrons and light-front sum rules in the $'t$ Hooft model," Phys. Rev. D **103**, 074002 (2021).

[15] P. Sun, X. B. Tong and F. Yuan, "Perturbative QCD analysis of near threshold heavy quarkonium photoproduction at large momentum transfer," Phys. Lett. B **822**, 136655 (2021).

[16] K. A. Mamo and I. Zahed, "Diffractive photoproduction of J/ψ and Υ using holographic QCD: gravitational form factors and GPD of gluons in the proton," Phys. Rev. D **101**, 086003 (2020).

[17] Y. Hatta, A. Rajan and D. L. Yang, "Near threshold J/ψ and Υ photoproduction at JLab and RHIC," Phys. Rev. D **100**, 014032 (2019).

[18] Y. Hatta and D. L. Yang, "Holographic J/ψ production near threshold and the proton mass problem," Phys. Rev. D **98**, 074003 (2018).

[19] Y. Guo, X. Ji and Y. Liu, "QCD Analysis of Near-Threshold Photon-Proton Production of Heavy Quarkonium," Phys. Rev. D **103**, 096010 (2021).

[20] X. Ji, "Proton mass decomposition: naturalness and interpretations," Front. Phys. (Beijing) **16**, 64601 (2021).

[21] D. Kharzeev, H. Satz, A. Syamtomov and G. Zinovjev, "J/ψ photoproduction and the gluon structure of the nucleon," Eur. Phys. J. C **9**, 459-462 (1999).

[22] P. Sun, X. B. Tong and F. Yuan, "Near threshold heavy quarkonium photoproduction at large momentum transfer," Phys. Rev. D **105**, no.5, 054032 (2022).

[23] A. Ali *et al.* [GlueX], "First Measurement of Near-Threshold J/ψ Exclusive Photoproduction off the Proton," Phys. Rev. Lett. **123**, 072001 (2019).

[24] D. P. Anderle, V. Bertone, X. Cao, L. Chang, N. Chang, G. Chen, X. Chen, Z. Chen, Z. Cui and L. Dai, *et al.* "Electron-ion collider in China," Front. Phys. (Beijing) **16**, 64701 (2021).

[25] A. Accardi, J. L. Albacete, M. Anselmino, N. Armesto, E. C. Aschenauer, A. Bacchetta, D. Boer, W. K. Brooks, T. Burton and N. B. Chang, *et al.* "Electron Ion Collider: The Next QCD Frontier: Understanding the glue that binds us all," Eur. Phys. J. A **52**, 268 (2016).

[26] J. Arrington, M. Battaglieri, A. Boehnlein, S. A. Bogacz, W. K. Brooks, E. Chudakov, I. Cloet, R. Ent, H. Gao and J. Grames, *et al.* "Physics with CEBAF at 12 GeV and future opportunities," Prog. Part. Nucl. Phys. **127**, 103985 (2022).

[27] X. Ji and Y. Liu, "Quantum anomalous energy effects on the nucleon mass," Sci. China Phys. Mech. Astron. **64**, 281012 (2021).

[28] D. Kharzeev, "Quarkonium interactions in QCD," Proc. Int. Sch. Phys. Fermi **130**, 105-131 (1996).

[29] K. A. Mamo and I. Zahed, "Nucleon mass radii and distribution: Holographic QCD, Lattice QCD and GlueX data," Phys. Rev. D **103**, no.9, 094010 (2021).

[30] X. B. Tong, J. P. Ma and F. Yuan, "Perturbative calculations of gravitational form factors at large momentum transfer," JHEP **10**, 046 (2022).

[31] V. Braun, R. J. Fries, N. Mahnke and E. Stein, "Higher twist distribution amplitudes of the nucleon in QCD," Nucl. Phys. B **589**, 381-409 (2000).

[32] V. M. Braun, A. Lenz and M. Wittmann, "Nucleon Form Factors in QCD," Phys. Rev. D **73**, 094019 (2006).

[33] P. A. Zyla *et al.* [Particle Data Group], "Review of Particle Physics," PTEP **2020**(8), 083C01 (2020).

[34] V. A. Novikov and M. A. Shifman, "Comment on the $\psi' \to J/\psi\pi\pi$ Decay," Z. Phys. C **8**, 43 (1981).

[35] X. D. Ji, "Lorentz symmetry and the internal structure of the nucleon," Phys. Rev. D **58**, 056003 (1998).

[36] T. J. Hou, J. Gao, T. J. Hobbs, K. Xie, S. Dulat, M. Guzzi, J. Huston, P. Nadolsky, J. Pumplin and C. Schmidt, *et al.* "New CTEQ global analysis of quantum chromodynamics with high-precision data from the LHC," Phys. Rev. D **103**, 014013 (2021).

[37] C. Alexandrou, S. Bacchio, M. Constantinou, J. Finkenrath, K. Hadjiyiannakou, K. Jansen, G. Koutsou, H. Panagopoulos and G. Spanoudes, "Complete flavor decomposition of the spin and momentum fraction of the proton using lattice QCD simulations at physical pion mass," Phys. Rev. D **101**, 094513 (2020).

[38] Y. B. Yang, J. Liang, Y. J. Bi, Y. Chen, T. Draper, K. F. Liu and Z. Liu, "Proton Mass Decomposition from the QCD Energy Momentum Tensor," Phys. Rev. Lett. **121**, , 212001 (2018).

[39] R. Fiore, L. Jenkovszky and M. Oleksiienko, "On Matter and Pressure Distribution in Nucleons," Phys. Part. Nucl. Lett. **18**, 5, 540-547 (2021).

[40] X. Y. Wang, F. Zeng and Q. Wang, "Systematic analysis of the proton mass radius based on photoproduction of vector charmoniums," Phys. Rev. D **105**, 096033 (2022).

[41] B. Gittelman, K. M. Hanson, D. Larson, E. Loh, A. Silverman and G. Theodosiou, "Photoproduction of the psi (3100) Meson at 11-GeV," Phys. Rev. Lett. **35**, 1616 (1975).

[42] U. Camerini, J. G. Learned, R. Prepost, C. M. Spencer, D. E. Wiser, W. Ash, R. L. Anderson, D. Ritson, D. Sherden and C. K. Sinclair, "Photoproduction of the ψ Particles," Phys. Rev. Lett. **35**, 483 (1975).

[43] P. L. Frabetti *et al.* [E687], "A Measurement of elastic J/ψ photoproduction cross-section at fermilab E687," Phys. Lett. B **316**, 197-206 (1993).

[44] M. J. Amarian, "Strangeness and charm production with HERMES," Few Body Syst. Suppl. **11**, 359-362 (1999)

[45] I. V. Anikin, "Gravitational form factors within light-cone sum rules at leading order," Phys. Rev. D **99**, 094026 (2019).

[46] P. Choudhary, B. Gurjar, D. Chakrabarti and A. Mukherjee, "Gravitational form factors and mechanical properties of the proton: Connections between distributions in 2D and 3D," Phys. Rev. D **106**, 076004 (2022).

[47] J. H. Jung, U. Yakhshiev, H. C. Kim and P. Schweitzer, "In-medium modified energy-momentum tensor form factors of the nucleon within the framework of a π-ρ-ω soliton model," Phys.

Rev. D **89**, 114021 (2014).

[48] H. Dutrieux, C. Lorcé, H. Moutarde, P. Sznajder, A. Trawiński and J. Wagner, "Phenomenological assessment of proton mechanical properties from deeply virtual Compton scattering," Eur. Phys. J. C **81**, 300 (2021).

[49] Z. F. Cui, D. Binosi, C. D. Roberts and S. M. Schmidt, "Hadron and light nucleus radii from electron scattering*," Chin. Phys. C **46**, no.12, 122001 (2022).

[50] Z. F. Cui, D. Binosi, C. D. Roberts and S. M. Schmidt, "Fresh Extraction of the Proton Charge Radius from Electron Scattering," Phys. Rev. Lett. **127**, 092001 (2021).